AIP | Journal of Applied Physics

# General expressions and physical origin of the coupling coefficient of arbitrary tuned coupled electromagnetic resonators

Sameh Y. Elnaggar, Richard J. Tervo, and Saba M. Mattar

Citation: Journal of Applied Physics **118**, 194901 (2015); doi: 10.1063/1.4935634
View online: http://dx.doi.org/10.1063/1.4935634
View Table of Contents: http://scitation.aip.org/content/aip/journal/jap/118/19?ver=pdfcov
Published by the AIP Publishing



# General expressions and physical origin of the coupling coefficient of arbitrary tuned coupled electromagnetic resonators

Sameh Y. Elnaggar,[1] Richard J. Tervo,[2] and Saba M. Mattar[3,a)]
[1]*School of Engineering and Information Technology, University of New South Wales, Canberra, Australia*
[2]*Department of Electrical and Computer Engineering, University of New Brunswick, Fredericton, NB, E3B 5A3 Canada*
[3]*Chemistry Department, University of New Brunswick, Fredericton, NB, E3B 5A3 Canada*

(Received 13 August 2015; accepted 1 November 2015; published online 16 November 2015)

The theory and operation of various devices and systems, such as wireless power transfer via magnetic resonant coupling, magneto-inductive wave devices, magnetic resonance spectroscopy probes, and metamaterials can rely on coupled tuned resonators. The coupling strength is usually expressed in terms of the coupling coefficient $\kappa$, which can have electrical $\kappa_E$ and/or magnetic $\kappa_M$ components. In the current article, general expressions of $\kappa$ are derived. The relation between the complex Poynting equation in its microscopic form and $\kappa$ is made and discussed in detail. It is shown that $\kappa$ can be expressed in terms of the interaction energy between the resonators' modes. It thus provides a general form that combines the magnetic and electric components of $\kappa$. The expressions make it possible to estimate the frequencies and fields of the coupled modes for arbitrarily oriented and spaced resonators. Thus, enabling the calculation of system specific parameters such as the transfer efficiency of wireless power transfer systems, resonator efficiency for electron spin resonance probes, and dispersion relations of magneto-inductive and stereo-metamaterials structures. © *2015 AIP Publishing LLC*. [http://dx.doi.org/10.1063/1.4935634]

## I. INTRODUCTION

To design efficient electron paramagnetic resonance (EPR) probes,[1–4] magneto-inductive devices,[5,6] wireless power transfer via inductively coupled resonators,[7–11] stereo-metamaterials,[12] and microwave filters,[13] it is essential to calculate and fully understand the coupling between its resonant components such as cavities, dielectric resonators, split-rings, micro-strips, and loop-gap resonators. The coupling coefficient $\kappa$ is the main parameter that quantifies the coupling strength. There are various definitions of $\kappa$ but they all revolve around the concept of energy exchange between resonators.[14,15] $\kappa$ has the effect of removing the degeneracy by splitting the frequencies of the coupled modes. It also appears as off-diagonal or non-secular terms in eigenvalue problems.

For lumped circuit models, the coupling mechanism is modelled by introducing a mutual capacitance ($C_m$) and/or inductance ($L_m$). Depending on the relative polarity of the mutual elements, the coupled frequency can be quantified by calculating $\kappa$[16,17]

$$\kappa = \kappa_M \pm \kappa_E = \frac{L_m}{L} \pm \frac{C_m}{C}. \tag{1}$$

Here $L$ and $C$ are the inductance and the capacitance of the uncoupled resonators, respectively. The sign between the two terms is determined by the relative orientation and structure of the resonators.

Expressing (1) in terms of the electromagnetic fields $\boldsymbol{E}$ and $\boldsymbol{H}$ is problematic. For example, Hong extended (1) by noticing that the mutual terms can be expressed by the overlap of the two corresponding fields. Thus, $C_m$ was replaced by $\int_V \epsilon \boldsymbol{E}_1^* \cdot \boldsymbol{E}_2 \, dv$ and $L_m$ by $\int_V \mu \boldsymbol{H}_1^* \cdot \boldsymbol{H}_2 \, dv$. The sign between the two terms was *chosen* to be positive,[18,19] i.e.,

$$\kappa = \kappa_M + \kappa_E \tag{2}$$

or

$$\kappa = \frac{\int_V \mu \boldsymbol{H}_1^* \cdot \boldsymbol{H}_2 \, dv + \int_V \epsilon \boldsymbol{E}_1^* \cdot \boldsymbol{E}_2 \, dv}{\sqrt{\int \epsilon |\boldsymbol{E}_1|^2 \, dv \times \int \epsilon |\boldsymbol{E}_2|^2 \, dv}}. \tag{3}$$

On the contrary, based on a coupled mode formalism, Awai and Zhang derived expressions for $\kappa$ which is in favor of using the negative sign,[15,20] i.e.,

$$\kappa = \kappa_M - \kappa_E \tag{4}$$

or

$$\kappa = \frac{\int_V \mu \boldsymbol{H}_1^* \cdot \boldsymbol{H}_2 \, dv - \int_V \epsilon \boldsymbol{E}_1^* \cdot \boldsymbol{E}_2 \, dv}{\sqrt{\int \epsilon |\boldsymbol{E}_1|^2 \, dv \times \int \epsilon |\boldsymbol{E}_2|^2 \, dv}}. \tag{5}$$

Using Lagrange's equation of motion, it was demonstrated that the interaction between two split-ring resonators, which form a meta-dimer, depends on the difference between the two terms. In this case, the coupled energy was expressed in terms of the surface charge and current densities.[21–23] Equations (2) and (4) cannot be assimilated together by merely changing the phase of the resonant modes.

As pointed out, (4) and (5) are valid for conducting resonators only. However, for dielectric resonators, $\kappa$ takes the form[15]

a)Electronic mail: mattar@unb.ca

 

$$\kappa = \frac{\int \epsilon_0(\epsilon_{r1}-1)\boldsymbol{E}_1^* \cdot \boldsymbol{E}_2\, dv}{\sqrt{\int \epsilon |\boldsymbol{E}_1|^2\, dv \times \int \epsilon |\boldsymbol{E}_2|^2\, dv}}. \quad (6)$$

The physical origin and general expressions for $\kappa$, which are valid for both conducting and dielectric resonators, have practical applications for scientists and engineers. For example, the ever increasing performance in the computational domain in terms of processing speed and storage makes it possible to numerically calculate the fields and frequencies of the modes of uncoupled resonators. The field values can be used to determine the coupling coefficients where the relative orientations of the resonators can be arbitrary and thus enables the study and design of complex systems. This is to be compared with lumped circuit models, where the calculation of $C_m$ and $L_m$ can be challenging and are usually complex functions of the resonators' positions and orientations.

Starting from Maxwell's equations, Energy Coupled Mode Theory (ECMT), a coupled mode formalism in the form of an eigenvalue problem, was derived. The eigenvalues and eigenvectors determine the coupled eigenmodes, which were proven to obey the resonance condition.[24] The method can be considered as the electromagnetic analog of Molecular Orbital Theory.[25] It was used to study an EPR probe which consists of a cavity with a dielectric insert.[2] In this interesting case, $\kappa$ of the dielectric $TE_{01\delta}$ and cavity $TE_{011}$ modes was found to be relatively large ($\approx$0.4). Moreover, expressions for fields-dependent parameters, such as the quality factor, filling factor, and probe efficiency, were obtained.[3,4] The interaction between the dielectric and cavity modes was later applied to design efficient EPR probes working at low temperatures (6 K).[26]

In the current article, ECMT is used to find general expressions for $\kappa$ which reduce to (4) and (6) when applied to conducting and dielectric resonators, respectively. Moreover, the physical origin of $\kappa$ follows naturally from the derived expressions.

This article is organized as follows: In Section II, the Poynting theorem is used to obtain useful relations which will be used in subsequent sections. The physical meaning of relevant terms is highlighted. Sections III, IV and V represents the basic foundations, where expressions of $\kappa$ are derived. In Section IV, the physical origin of $\kappa$ is discussed. Section V applies the derived expressions to different cases and scenarios. Finally, the conclusions follow in Section VI.

## II. THEORETICAL BACKGROUND

In the current article, the inner product of two vector fields is formulated using Dirac bra-ket notation. For example, the inner product of $\boldsymbol{A}$ and $\boldsymbol{B}$ is denoted by $\langle \boldsymbol{A}|\boldsymbol{B}\rangle$ and is defined by

$$\langle \boldsymbol{A}|\boldsymbol{B}\rangle \equiv \int_V \boldsymbol{A}^* \cdot \boldsymbol{B}\, dv,$$

where $V$ is the total volume and $K^*$ is the complex conjugate of $K$. Clearly $\langle \boldsymbol{A}|\boldsymbol{B}\rangle^* = \langle \boldsymbol{B}|\boldsymbol{A}\rangle$.

The dielectric constant of resonator $u$ is a function of the spatial coordinates and is denoted by $\epsilon_u$. For two coupled resonators 1 and 2, the coupled dielectric constant is denoted by $\epsilon$ and is equal to max ($\epsilon_1$, $\epsilon_2$).

### A. Energy interaction terms

Since coupling primarily depends on reactive components (for example, in lumped circuit models it depends on $C_m$ and $L_m$), only the reactive fields are considered. As previously mentioned, the concept of coupling revolves around the "*energy*" keyword. Thus, it is convenient to start from the conservation of energy. Because ECMT is formulated in the frequency domain, the complex Poynting theorem is used,[27]

$$-\frac{1}{2}\int_{\partial V} \boldsymbol{E}\times\boldsymbol{H}^* \cdot d\boldsymbol{S} - \frac{1}{2}\langle \boldsymbol{J}|\boldsymbol{E}\rangle = 2j\omega(\langle W_M\rangle - \langle W_E\rangle). \quad (7)$$

Here $\langle W_M\rangle$ and $\langle W_E\rangle$ are the average magnetic and electric stored energy, respectively. It is useful to re-write (7) in terms of the maximum stored energy. Thus,

$$-\frac{T}{4\pi}\left(\int_{\partial V} \boldsymbol{E}\times\boldsymbol{H}^* \cdot d\boldsymbol{S} + \langle \boldsymbol{J}|\boldsymbol{E}\rangle\right) = j(\max(W_M) - \max(W_E)), \quad (8)$$

where $T = 2\pi/\omega$ is the oscillation period. The energy term $\max(W_E)$ takes into account the energy stored in the dipole moments (i.e., (8) is in the macroscopic form).[28] The contribution of the materials, represented by the electric dipole $\boldsymbol{P} = \epsilon_0(\epsilon_r - 1)\boldsymbol{E}$, can be separated from $\max(W_E)$, thus leading to the microscopic form of the Poynting theorem

$$-\frac{T}{4\pi}\left(\int_{\partial V} \boldsymbol{E}\times\boldsymbol{H}^* \cdot d\boldsymbol{S} + \langle \boldsymbol{J}|\boldsymbol{E}\rangle\right) + \frac{j}{2}\langle \boldsymbol{P}|\boldsymbol{E}\rangle = j\left(\max(W_M) - \max\left(W_E^0\right)\right), \quad (9)$$

where $\max(W_E^0) = \frac{1}{2}\langle \epsilon_0\boldsymbol{E}|\boldsymbol{E}\rangle$ is the electric energy stored in free space. $(-T/4\pi)\int_{\partial V}\boldsymbol{E}\times\boldsymbol{H}^*\cdot d\boldsymbol{S}$ is the maximum energy entering the volume $V$ (it can also be regarded as the energy due to the equivalent current sheet $\hat{n}\times\boldsymbol{H}$), $-(T/4\pi)\langle \boldsymbol{J}|\boldsymbol{E}\rangle$ is the maximum energy that the current $\boldsymbol{J}$ exerts on the system, and $-\langle \boldsymbol{P}|\boldsymbol{E}\rangle$ is the maximum potential energy (PE) stored in the moment $\boldsymbol{P}$.

As will be seen later in Section III, the $\kappa$ expressions are strongly related to the microscopic form (9). To better understand (9), correspondence relations with a frictionless mass-spring system driven by a sinusoidal force, $F_D = F_0 \sin\omega t$, have been made. A full and detailed discussion, relevant to the present analysis, of the frictionless mass-spring system is given in the Appendix. Equations (8) and (9) are similar to the work energy relationship (A4). The magnetic energy $W_M$ corresponds to the $PE$, $W_E^0$ corresponds to the kinetic energy ($KE$), and the reactive energy $-(T/4\pi)(\int_{\partial V}\boldsymbol{E}\times\boldsymbol{H}^*\cdot d\boldsymbol{S} + \langle \boldsymbol{J}|\boldsymbol{E}\rangle)$ is equivalent to the reactive work exerted by or on the source ($\int_{x(t=0)}^{x(t=T/4)} F_D dx$). Noting that there is a 90° phase shift between $W_M$ and $W_E^0$, (9) can be explained as follows: The energy oscillates between the magnetic and electric fields. After quarter of a cycle, the maximum magnetic energy $\max(W_M)$ is converted into three main components. The first is the electric energy stored in $V$, $\max(W_E^0)$. The second

component is the energy returned to the equivalent sources $-(T/4\pi)(\int_{\partial V}\boldsymbol{E}\times\boldsymbol{H}^*\cdot d\boldsymbol{S}+\langle\boldsymbol{J}|\boldsymbol{E}\rangle)$. The third is the electric energy stored in the dielectric material $1/2(\langle\boldsymbol{P}|\boldsymbol{E}\rangle)$. Fig. 1 depicts a hypothetical system which has a dielectric material ($\boldsymbol{P}$) and a current element ($\boldsymbol{J}$). As mentioned above, the energy crossing the boundary $\partial V$, can be considered as the interaction of the electric field $\boldsymbol{E}$ and an equivalent current sheet $\hat{n}\times\boldsymbol{H}$. This energy component can be set to zero if the volume is large. In another words, the total reactive field is enclosed in $V$.

### B. Energy cross terms

According to ECMT, the electric and magnetic fields of the coupled system are the superposition of the uncoupled fields, i.e.,

$$\boldsymbol{E}=\sum_{u=1}^{N}a_u\boldsymbol{E}_u \tag{10}$$

and

$$\boldsymbol{H}=\sum_{u=1}^{N}b_u\boldsymbol{H}_u. \tag{11}$$

Using (10) and (11), the energy terms in (9) can be written as

$$\int_{\partial V}\boldsymbol{E}\times\boldsymbol{H}^*\cdot d\boldsymbol{S}=a^t\mathcal{M}^*b^*, \tag{12}$$

$$\langle\boldsymbol{J}|\boldsymbol{E}\rangle=b^\dagger\mathcal{N}^*a, \tag{13}$$

and

$$\langle\boldsymbol{P}|\boldsymbol{E}\rangle=a^*\mathcal{P}a. \tag{14}$$

Here $\mathcal{M}_{uv}=\int_{\partial V}\boldsymbol{E}_u^*\times\boldsymbol{H}_v\cdot d\boldsymbol{S}$, $\mathcal{N}_{uv}=\langle\boldsymbol{E}_u|\boldsymbol{J}_v\rangle$ (Ref. 24) and $\mathcal{P}_{uv}=\langle\boldsymbol{P}_u|\boldsymbol{E}_v\rangle$. For non-magnetic media, if $\mathcal{G}_{uv}\equiv\langle\mu_0\boldsymbol{H}_u|\boldsymbol{H}_v\rangle$ and $\mathcal{D}_{uv}\equiv\langle\epsilon_u\boldsymbol{E}_u|\boldsymbol{E}_v\rangle$, it was shown that[24]

$$\mathcal{M}_{uv}+\mathcal{N}_{uv}=j\omega_0(\mathcal{G}_{uv}-\mathcal{D}_{vu}^*). \tag{15}$$

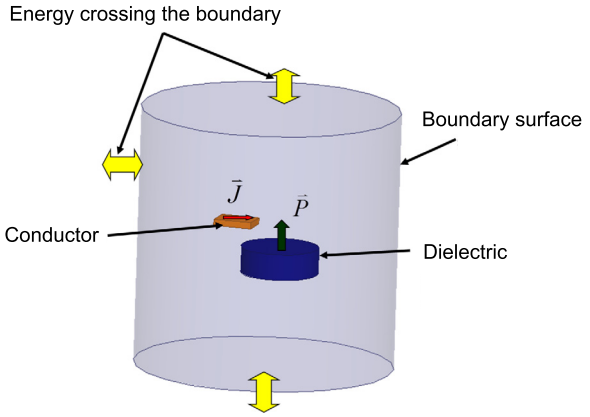


FIG. 1. A system which contains dielectric and conducting components. The energy is stored in various components as well as crossing the boundary surface.

Expanding the stored energy terms $W_M$ and $W_E$ in terms of the uncoupled fields given by (10) and (11) and using (15), it can be shown that

$$j\frac{T}{4\pi}\left(\mathcal{M}_{uv}^*+\mathcal{N}_{vu}^*\right)+\frac{1}{2}\mathcal{P}_{vu}=\left[\max(W_M)_{vu}-\max(W_E)_{vu}^0\right], \tag{16}$$

where $\max(W_M)_{vu}=\frac{1}{2}\langle\mu_0\boldsymbol{H}_k|\boldsymbol{H}_i\rangle$ and $\max(W_E)_{vu}^0=\frac{1}{2}\langle\epsilon_0\boldsymbol{E}_v|\boldsymbol{E}_u\rangle$ are the ($u$, $v$) free space magnetic and electric coupled energy components, respectively.

## III. ANALYSIS

In this section and based on ECMT, general expressions for the coupling coefficient of two tuned coupled resonators are derived. For the coupled system, the eigenvalue problem of two tuned (degenerate) resonators can be written as[24]

$$\omega_0^2\mathcal{A}^{-1}\mathcal{D}^\dagger\mathcal{G}^{-1}\mathcal{D}a=\omega^2a, \tag{17}$$

where $\mathcal{A}_{uv}\equiv\langle\epsilon\boldsymbol{E}_u|\boldsymbol{E}_v\rangle=2\max(W_E)_{uv}$ and $\omega_0$ is the uncoupled angular frequency. Usually for weakly coupled resonators, $\mathcal{A}_{11}\mathcal{A}_{22}\gg\mathcal{A}_{12}\mathcal{A}_{21}$, $\mathcal{G}_{11}\mathcal{G}_{22}\gg\mathcal{G}_{12}\mathcal{G}_{21}$, and $\mathcal{A}_{uu}\approx\mathcal{D}_{uu}\approx\mathcal{G}_{uu}$. These approximations simplify the eigenvalue equation (17) to

$$\begin{pmatrix}\omega_0^2 & \omega_0^2\dfrac{\mathcal{D}_{12}-\mathcal{G}_{12}+\mathcal{D}_{21}^*-\mathcal{A}_{12}}{\mathcal{A}_{11}}\\ \omega_0^2\dfrac{\mathcal{D}_{21}-\mathcal{G}_{21}+\mathcal{D}_{12}^*-\mathcal{A}_{21}}{\mathcal{A}_{22}} & \omega_0^2\end{pmatrix}a=\omega^2a. \tag{18}$$

The coupling coefficient $\kappa$ is the negative of the off diagonal term divided by the on diagonal one. In lumped circuits this is equal to $C_m/\sqrt{C_1C_2}$ or $L_m/\sqrt{L_1L_2}$ ($C_i$ and $L_i$ are the capacitance and inductance of the ith resonator, respectively). In the case at hand $\kappa$ is equal to

$$\kappa_{uv}=-\frac{\mathcal{D}_{uv}-\mathcal{G}_{uv}+\mathcal{D}_{vu}^*-\mathcal{A}_{uv}}{\mathcal{A}_{uu}}, \tag{19}$$

where $\mathcal{D}_{uv}+\mathcal{D}_{vu}^*-\mathcal{A}_{uv}=\int_V(\epsilon_u+\epsilon_v-\epsilon)\boldsymbol{E}_u^*\cdot\boldsymbol{E}_v\,dv=\int_V\epsilon_{bg}\boldsymbol{E}_u^*\cdot\boldsymbol{E}_v\,dv$ and losses are ignored. Here $\epsilon_{bg}\equiv\epsilon_u+\epsilon_v-\epsilon$ is the background dielectric profile. Therefore, the coupling coefficient of any two arbitrary tuned resonators is

$$\kappa_{uv}=\frac{\int_V\left(\mu_0\boldsymbol{H}_u^*\cdot\boldsymbol{H}_v-\epsilon_{bg}\boldsymbol{E}_u^*\cdot\boldsymbol{E}_v\right)dv}{\int_V\epsilon|\boldsymbol{E}_u|^2\,dv}. \tag{20}$$

Expression (20) looks similar to (4) and (5) derived for conducting resonators.[15] However, (20) depends on the background permittivity which, as will be shown in Sections IV and V, makes (20) general and valid for any type of resonators. Moreover, the right hand side of (20) proves that for normalized modes (the modes amplitudes are chosen such that $\mathcal{A}_{uu}=\mathcal{A}_{vv}$), $\kappa_{uv}$ and $\kappa_{vu}$ form a conjugate pair, i.e.,

$$\kappa_{uv}=\kappa_{vu}^*. \tag{21}$$

## IV. PHYSICAL ORIGIN OF THE COUPLING COEFFICIENT

Although (20) is general and can be used to calculate $\kappa$ for arbitrary resonators, it does not explicitly show the energy interaction terms as described by (9) and (16). To express $\kappa$ in terms of energy components, (15) is used. Thus for normalized modes, (19) is re-written as

$$\kappa_{uv} = \frac{\mathcal{P}_{uv}/2 + jT/4\pi\left(\mathcal{M}^*_{vu} + \mathcal{N}^*_{vu}\right)}{\max(W_E)_{uu}}. \tag{22}$$

Equation (22) reveals the physical origin of $\kappa_{uv}$. The coupling coefficient $\kappa_{uv}$ is then equal to the maximum work that the elements ($\boldsymbol{P}_u$, $\hat{n} \times \boldsymbol{H}_u|_{\partial V}$ and $\boldsymbol{J}_u$) of resonator $u$ exerts on resonator $v$. This is valid regardless of the type of resonators (dielectric, conducting or both).

It is worthy of notice that (20) and (22) are valid for wide ranges of frequencies. The eigenvalue problem (17) was obtained for arbitrary resonators with an arbitrary angular frequency $\omega$. It was shown that accurate values of the coupled frequencies and fields can be obtained up to the sub-millimeter regime when the quality factors are relatively low due to radiation.[24] For higher frequencies, particularly when the resonant frequencies are close to the plasma frequency, at which $\epsilon$ and hence $\mathcal{A}$ are strong functions of $\omega$, the solution of (17) will be more involved.

## V. RESULTS AND DISCUSSION

In the following, the equivalent general expressions (19), (20), and (22) will be applied to different systems. The results will be compared with Finite element simulations and other results found in the literature. Without loss of generality, the volume $V$ is taken to be large enough such that $\mathcal{M}_{uv} \approx 0$. In this case (22) can be written as

$$\kappa_{uv} = \frac{\mathcal{P}_{uv}/2 + jT/4\pi\mathcal{N}^*_{vu}}{\mathcal{A}_{uu}/2}. \tag{23}$$

### A. Coupling between conducting resonators

Conducting resonators appear in various systems and devices. For example split-ring resonators are the building blocks of metamaterials.[29] They are also used in filters.[19] Loop-gaps are used to enhance the signal of EPR probes.[30] The common theme here is that $\boldsymbol{P}_{uv} = 0$. In such cases $\epsilon_{bg} = \epsilon_0$ and from (20)

$$\kappa_{uv} = \kappa^*_{vu} = \frac{\int_V (\mu_0 \boldsymbol{H}^*_u \cdot \boldsymbol{H}_v - \epsilon_0 \boldsymbol{E}^*_u \cdot \boldsymbol{E}_v)\, dv}{\int_V \boldsymbol{E}^*_u \cdot \boldsymbol{E}_u\, dv}, \tag{24}$$

which is equivalent to the formula derived using Coupled Mode Theory[15,20] and Lagrange's equation of motion.[22] The difference between the two terms in the numerator of (24) was previously attributed to the counter effect of the magnetic and electric dipole moments.[31,32] As was previously shown[24] and according to (23), the coupling is the result of the interaction of the fields of resonator $u$ with the current of resonator $v$. Equation (24) was previously verified for different structures.[15,22] To reinforce the validity of (24), $\kappa$ of the two tuned loop-gap resonators, shown in the inset of Fig. 2, is calculated for different separation distances $d$. The results are then compared with the formula found in Ref. 19 ($\kappa = \kappa_M + \kappa_E$) and to the frequency splitting formula

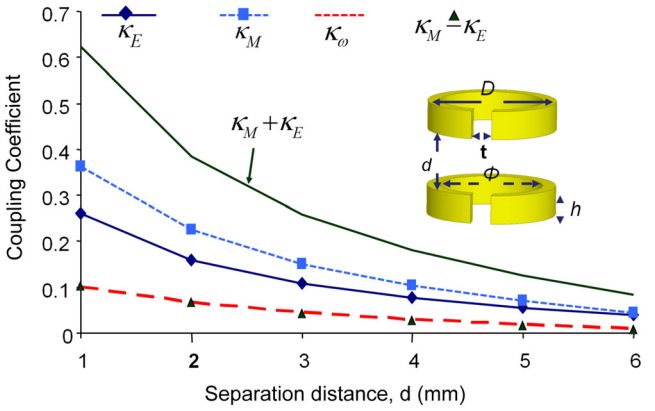


FIG. 2. The coupling coefficient calculated for two coupled loop gap resonators. The uncoupled frequency of each resonators is 9.79 GHz. The outer diameter $D = 5$ mm, inner diameter $\phi = 4$ mm, height $h = 1$ mm, and gap thickness $t = 0.8$ mm.

$$\kappa_\omega = \frac{\omega^2_{+-} - \omega^2_{++}}{\omega^2_{+-} + \omega^2_{++}}. \tag{25}$$

The symmetric and anti-symmetric angular frequencies ($\omega_{++}$ and $\omega_{+-}$) are calculated using the HFSS® Eigenmode solver (Ansys Corporation, Pittsburgh, PA, USA). Using the solver, the resonant frequency and fields of the single, uncoupled loop gap were computed and exported into a MATLAB® code which calculates the overlap integrals in (24). Fig. 2 verifies that $\kappa$ is the difference between $\kappa_M$ and $\kappa_E$. Because the electric field is concentrated in the gaps, $\kappa_E$ is always smaller than $\kappa_M$. When $d$ increases, both terms monotonically decrease and approaches zero. However, for a finite distance $d$, the condition: $\kappa_M = \kappa_E$ will never be satisfied.

To achieve the condition $\kappa_M = \kappa_E$, the eigenmodes of two tuned coplanar double split ring resonators, shown in Fig. 3, are computed. This arrangement makes it possible to scan for the angle $\phi$ at which $\kappa = 0$.

When $\phi = 0°$ or $\phi = 90°$, the coupling is strong. Figs. 4 and 5 show the coupled surface current density for both cases.

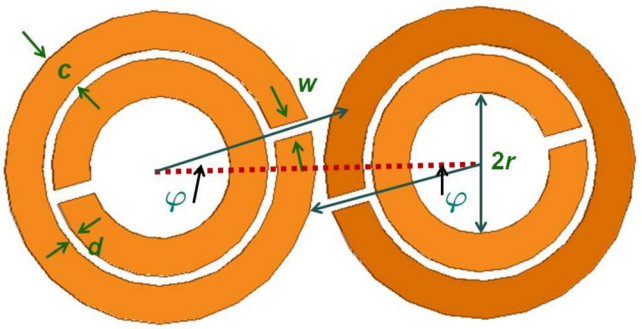


FIG. 3. Two tuned coupled double split ring resonators. $d = 0.2$ mm, $c = 0.8$ mm, $r = 1.5$ mm, $w = 0.3$ mm, $t = 50\ \mu$m, and the resonant frequency $f_0 \approx 4.8$ GHz.

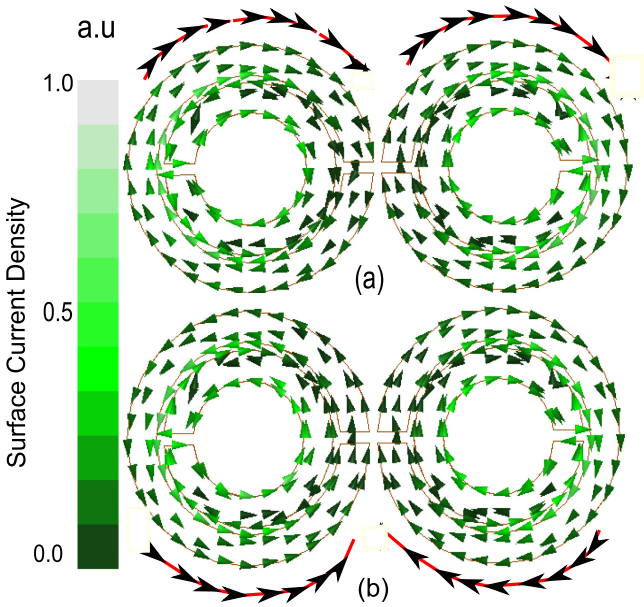


FIG. 4. The surface current density of the (top) symmetric mode and (bottom) anti-symmetric mode of two tuned coupled split ring resonators for an angle $\phi = 0°$.

The linearity of Maxwell's equations makes it possible to scale the fields of the eigenmodes by multiplying them by an arbitrary complex number. Hence the values in Figs. 4 and 5 are expressed in arbitrary units. It is worth mentioning that the difference in the current direction in Figs. 4 and 5 (180° phase shift) is due to the complex number multiplication and has no effect on the analysis, since the ratio of the amplitudes and difference in phases between any two given points are always preserved. For the $\phi = 0°$ situation (Fig. 4), the coupling is predominately electric due to the overlap of $\boldsymbol{E}_1$ and $\boldsymbol{E}_2$. On the contrary, it is predominately magnetic when $\phi = 90°$

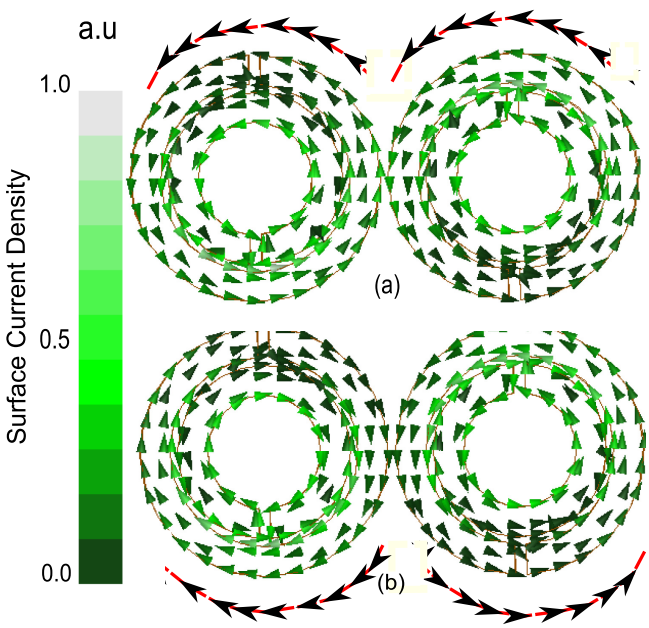


FIG. 5. The surface current density of the (top) symmetric mode and (bottom) anti-symmetric mode of two tuned coupled split ring resonators for an angle $\phi = 90°$.

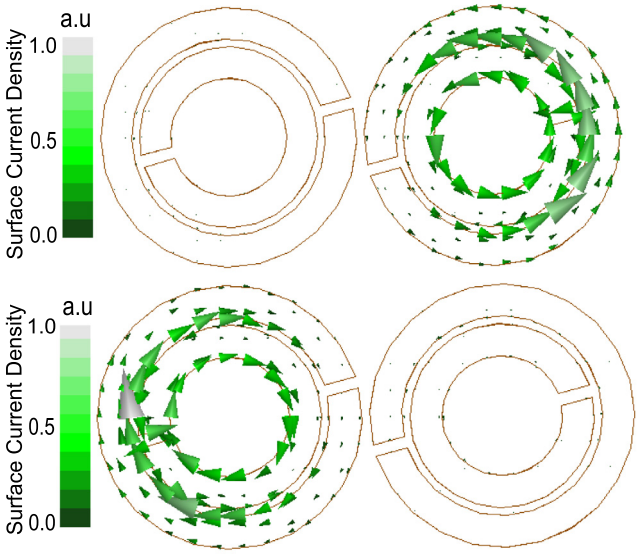


FIG. 6. The surface current density (top) of the symmetric (bottom) and the anti-symmetric modes due to the coupling of two tuned coupled double split ring resonators when $\phi = 15°$.

(Fig. 5). The symmetric mode corresponds to the situation where the two modes are in phase.[2] Thus, the currents on all rings circulate in the same direction, as the arrows in Figs. 4 and 5 show. This has the effect of an enhanced magnetic dipole (top plots in Figs. 4 and 5). Accordingly, the mode can be coupled to an external electromagnetic wave via the magnetic field component orthogonal to the rings plane. On the contrary for the antisymmetric mode, the currents on the rings circulate in opposite directions (bottom plots in Figs. 4 and 5) and thus the mode has a zero net magnetic dipole and can couple to the external electromagnetic wave via the net electric dipole moment in the gaps. Therefore, it can be deduced that the symmetric (antisymmetric) mode corresponds to a magnetic (electric) type resonance.[33,34] Unlike the situation depicted in Fig. 2 at some rotation angle $\phi_0$, $\kappa$ vanishes. Using the finite element simulation, we found that $\phi_0 = 15°$. At this angle, the symmetric and anti-symmetric modes decouple as Fig. 6 presents.

The physical origin of why the *decoupling* between the two resonators occurs can be revealed by referring to (23). Noting that $\mathcal{P}_{uv} = 0$, $\kappa$ can be written as

$$\kappa = j\frac{T/4\pi\langle \boldsymbol{J}_u|\boldsymbol{E}_v\rangle}{\mathcal{A}_{uu}/2}. \tag{26}$$

The decoupling occurs when $\kappa = 0$ or, equivalently, the electric field of resonator $u$ is orthogonal to the surface current of resonator $u$ ($\langle \boldsymbol{J}_u|\boldsymbol{E}_v\rangle = 0$). In another words, there is no interaction between the two resonators. This is true even though $\kappa_E$ and $\kappa_M \neq 0$.

### B. Coupling between two dielectric resonators

In this subsection, an expression for $\kappa$ due to the coupling of two dielectric resonators is derived and then used to calculate the coupled frequencies ($\omega_{++}$ and $\omega_{+-}$). For

purely dielectric resonators, $\boldsymbol{J}=0$. Therefore according to (23), $\kappa_{uv}$ can be expressed as

$$\kappa_{uv}=\frac{\mathcal{P}_{uv}}{\mathcal{A}_{uu}}=\frac{\int_{V_v}(\epsilon_u(\boldsymbol{r})-1)\boldsymbol{E}_u^*\cdot\boldsymbol{E}_v dv}{\int_V \epsilon|\boldsymbol{E}_u|^2 dv}. \tag{27}$$

Equation (27) agrees with the findings of Refs. 15 and 35. As a further verification of (27) and the coupled mode equation (17), the symmetric and anti-symmetric frequencies due to the coupling of the dielectric resonators $TE_{01\delta}$ modes are calculated and compared to High Frequency Structural Simulator (HFSS) simulations as shown in Fig. 7.

The agreement between the frequencies calculated using ECMT and finite element simulations verifies the validity of (17) and (27). For the configuration depicted in Fig. 7, $\kappa$ does not vanish for any finite distance $d$. However, if the coupling is between the $TE_{01\delta}$ mode of one dielectric resonator and the higher order mode of the other resonator, $\langle \boldsymbol{E}_v|\boldsymbol{E}_u\rangle$ may vanish.

### C. Coupling between a dielectric and a conducting resonators

As a final example, an expression for $\kappa$ due to the coupling between a dielectric resonator and a cavity is obtained. Hereafter, the dielectric resonator is labelled as *Resonator 1* and the cavity as *Resonator 2*. Applying (23) and noting that $\mathcal{P}_{21}=0$ and $\mathcal{N}_{21}=0$, one can find that

$$\kappa_{12}=\frac{\mathcal{P}_{12}^*}{\mathcal{A}_{11}} \tag{28}$$

and

$$\kappa_{21}=\frac{j}{\omega_0}\frac{\langle \boldsymbol{J}_2|\boldsymbol{E}_1\rangle}{\mathcal{A}_{11}}. \tag{29}$$

Although (28) and (29) look different, basically they have the same magnitude (refer to Eq. (21)). This means that the interaction energy between the dielectric dipole vector $\epsilon_0(\epsilon_r-1)\boldsymbol{E}_1$ and the cavity electric field $\boldsymbol{E}_2$ is the same as the energy due to the coupling of $\boldsymbol{E}_1$ and the surface current on the cavity walls. Figs. 8 and 9 depict the relevant fields when the interaction is between the dielectric's $TE_{01\delta}$ and the cavity's $TE_{011}$ modes. Due to the reciprocity relation (21), any of the two formulas (28) or (29) can be used to determine the coupled modes. However, it might be more convenient to use one formula than the other. For instance, the electric field $\boldsymbol{E}_1$ of the $TE_{01\delta}$ can be estimated using the Cohn Model.[2,36] The main assumption of the Cohn model is that the dielectric resonator is held inside a magnetic wall waveguide and thus ignores the diffraction of the fields as they extend outside the dielectric material. Hence, the estimated fields are not accurate outside the dielectric material. Accordingly, it is more convenient to use (29) because the calculated $\boldsymbol{E}_1$ is already available.

Table I presents the calculated frequencies of the symmetric and anti-symmetric modes which result from the coupling of a cylindrical cavity $TE_{011}$ and dielectric resonator $TE_{01\delta}$ modes. The calculation is carried out using two dielectric resonators. The first is with a moderate $\epsilon_r$, while the other has a very high dielectric constant ($\epsilon_r=261$). From the table, it is clear that treating the coupling as an interaction between

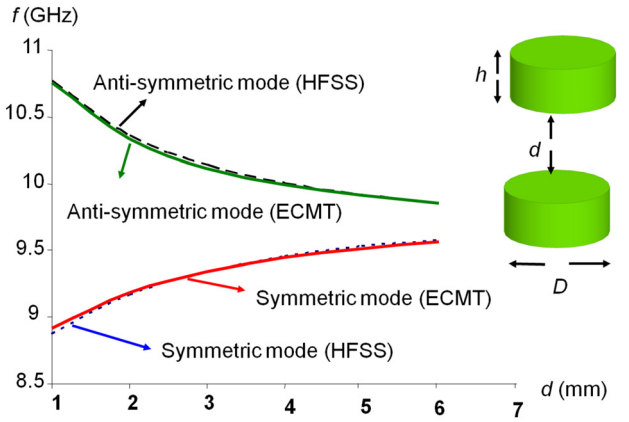


FIG. 7. The frequencies of the symmetric and anti-symmetric modes due to the coupling between two dielectric resonators. $\epsilon_r=29.2$, $h=2.65$ mm, and $D=6$ mm. The resonant frequency of the single dielectric resonator is $f_0\approx 9.7$ GHz.

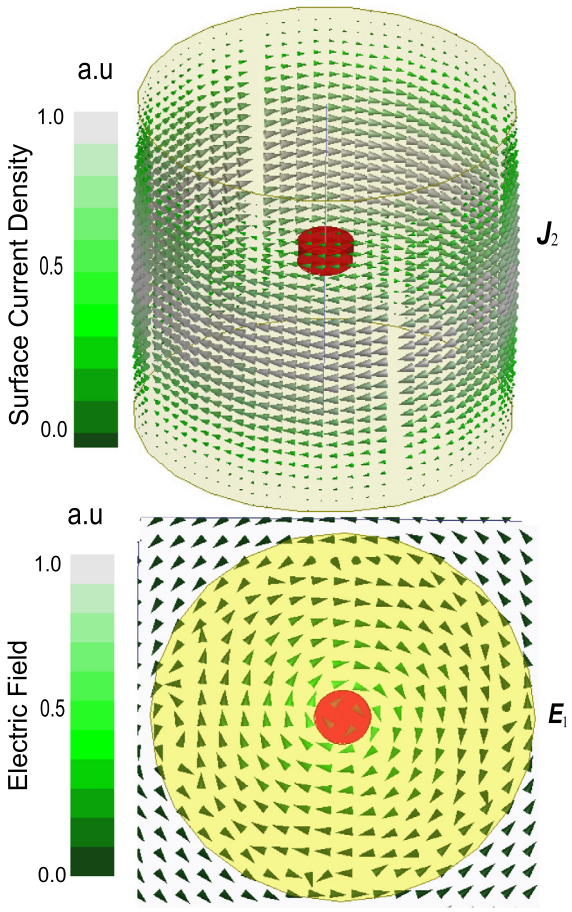


FIG. 8. Top: The surface current $\boldsymbol{J}_2$ of the cylindrical cavity's $TE_{011}$ mode. Bottom: The electric field $\boldsymbol{E}_1$ of the dielectric resonator's $TE_{01\delta}$ mode. Cavity Dimension: Height = Diameter = 4.1 cm, $f_{TE011}=9.7$ GHz. Dielectric Dimension: Height = 2.65 mm, Diameter = 6 mm. $f_{TE01\delta}=9.7$ GHz. $\epsilon_r=29.2$.

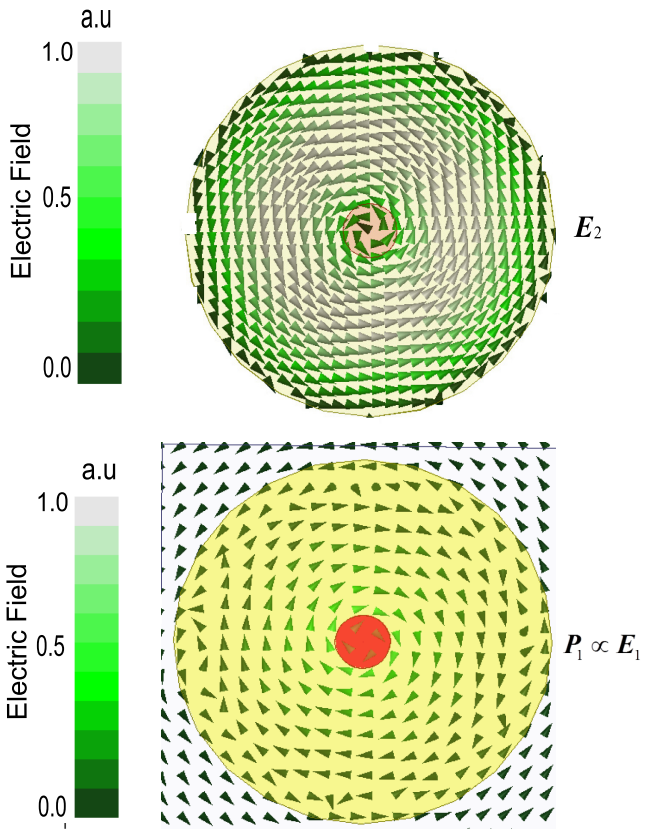


FIG. 9. Top: The electric field $\boldsymbol{E}_2$ of the cylindrical cavity's $TE_{011}$ mode. Bottom: The electric field $\boldsymbol{E}_1$ of the dielectric resonator's $TE_{01\delta}$ mode. Cavity Dimension: Height = Diameter = 4.1 cm, $f_{TE011}$ = 9.7 GHz. Dielectric Dimension: Height = 2.65 mm, Diameter = 6 mm. $f_{TE01\delta}$ = 9.7 GHz. $\epsilon_r = 29.2$.

TABLE I. The frequency of the symmetric and anti-symmetric modes which result from the coupling of the dielectric resonator $TE_{01\delta}$ and the cylindrical cavity $TE_{011}$ modes. The dielectric diameter and height are denoted by $D$ and $h$, respectively. The dimensions of the dielectric resonator and the cavity were chosen such that the $TE_{011}$ and $TE_{01\delta}$ modes have the same frequency.

| | | | Frequency (GHz) | | | |
|---|---|---|---|---|---|---|
| | | | Symmetric | | Anti-symmetric | |
| $\epsilon_r$ | $D$ (mm) | $h$ (mm) | ECMT | HFSS | ECMT | HFSS |
| 29.2 | 6 | 2.65 | 9.201 | 9.209 | 10.374 | 10.417 |
| 261 | 1.75 | 1.75 | 9.476 | 9.482 | 9.679 | 9.735 |

the polarization vector and the electric field enables us to accurately calculate the frequency values.

## VI. CONCLUSION

Using ECMT, general expressions of the coupling coefficient $\kappa$ between tuned coupled resonators are derived. When the complex Poynting theorem is used, the physical origin of $\kappa$ becomes clear. It is shown that $\kappa_{uv} = \kappa_{vu}^*$ for arbitrary tuned coupled resonators. Moreover, $\kappa$ depends on the interaction of one resonator with the other's equivalent sources ($\boldsymbol{P}$, $\boldsymbol{J}$ and $\hat{n} \times \boldsymbol{H}|_{\partial V}$). The general expressions of $\kappa$ reduce to well-known formulas which were derived for certain types of resonators. $\kappa$ and/or the coupled frequencies were calculated for different configurations used in magnetic resonance spectroscopy and metamaterials (loop-gaps, bridged loop-gaps, double split rings, dielectric resonators, and cavities containing dielectric resonators). It was shown that when the equivalent sources of one resonator are orthogonal to fields of the other, the two resonators do not interact. This is true even if the resonators are in a very close proximity to one another. The expressions derived here are valid for different resonators which can be arbitrarily oriented in space. Thus, it can aid in the analysis of the of wireless power transfer systems, EPR probes, metamaterial media, and magneto-inductive waves and devices.

It is essential to compare the current approach with other approaches reported in the literature to illustrate the usefulness of the current methodology. Expressions (20) and (22) were directly derived from (17) which in turn was obtained from Maxwell's equations under the assumption that the modes are hybridized. As mentioned above, the coupling coefficient $\kappa = \kappa_M - \kappa_E$ is reduced to the interaction energies of the equivalent sources ($\boldsymbol{P}$, $\boldsymbol{J}$ and $\hat{n} \times \boldsymbol{H}|_{\partial V}$). Thus, there is no need to determine the magnitude and polarity of the mutual inductance and/or capacitance. The current approach treats dielectric and conducting resonators on the same footing. The physical origin of the modes decoupling phenomenon (whenever $\kappa_M = \kappa_E$) follows directly from the proposed physical explanation of $\kappa$. Other approaches, whether based on the solution of the Lagrangian equation of motion or lumped circuit models, have been successfully applied to particular configurations involving split ring resonators.[5,12,21,23,37] The counter effect of $\kappa_M$ and $\kappa_E$ was attributed to the opposite contributions of the electric-electric and magnetic-magnetic dipoles.[12,24] However, generalization to cover situations where dielectric and dielectric/conducting resonators is not straightforward.

## ACKNOWLEDGMENTS

S.M.M. acknowledges the Natural Sciences and Engineering Research Council of Canada for financial support in the form of a discovery (operating) grant. S.Y.N. is grateful for the financial assistance from the University of New Brunswick in the form of pre-doctoral teaching and research assistantships. We would also like to acknowledge CMC Microsystems for providing HFSS® that facilitated this research.

## APPENDIX: FRICTIONLESS MASS-SPRING SYSTEM

The energy conversation of a frictionless, mass-spring system driven by a sinusoidal force, $F_D = F_0 \sin \omega t$, shown in Fig. 10, is studied in detail. For the mass-spring system one can write the governing equation as

$$\frac{d^2x}{dt^2} + \omega_0^2 x = \frac{F_D}{m} = \frac{F_0}{m} \sin \omega t, \tag{A1}$$

where $x$ is the elongation of the spring, $m$ is the mass, $F_0$ is the amplitude of the driving force, and $\omega_0$ is the natural frequency which is equal to $\sqrt{\frac{k}{m}}$, where $k$ is the spring constant.

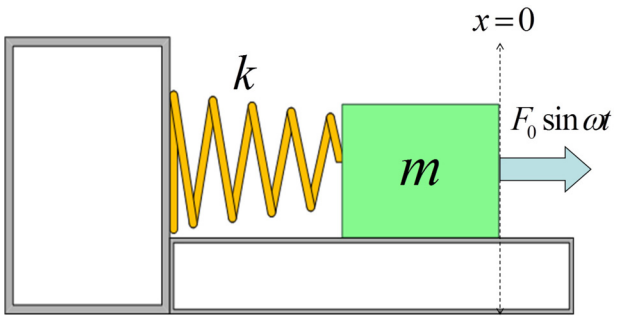


FIG. 10. Frictionless mass spring system driven by a sinusoidal force.

Taking $x = 0$ when $t = 0$ as the reference point, the forced response of (A1) is

$$x(t) = \frac{F_0}{m(\omega_0^2 - \omega^2)} \sin \omega t. \tag{A2}$$

The work-energy equation for the lossless mass-spring system can be written as

$$\int_{(1)}^{(2)} F_D dx = (KE_2 + PE_2) - (KE_1 + PE_1). \tag{A3}$$

The right hand side of (A3) is the difference in total energy $KE + PE$ between point (2) and point (1), while the left hand side is the work done by the driving source. Taking point (2) to be the point where $PE = 0$, $\left(t = \frac{T}{4}, \frac{dx}{dt} = 0\right)$, and point (1) to be the point where $KE = 0$, $(t = 0, x = 0)$, one can rewrite the work-energy equation (A3) as

$$\int_{x(t=0)}^{x(t=T/4)} F_D dx = \max(PE) - \max(KE) = \frac{F_0^2}{2m(\omega_0^2 - \omega^2)}. \tag{A4}$$

The work term $\int_{x(t=0)}^{x(t=T/4)} F_D dx$ is reactive. This means that the energy supplied by the source for quarter of a cycle returns back to it in the next quarter cycle. Indeed this can be understood by examining the instantaneous power

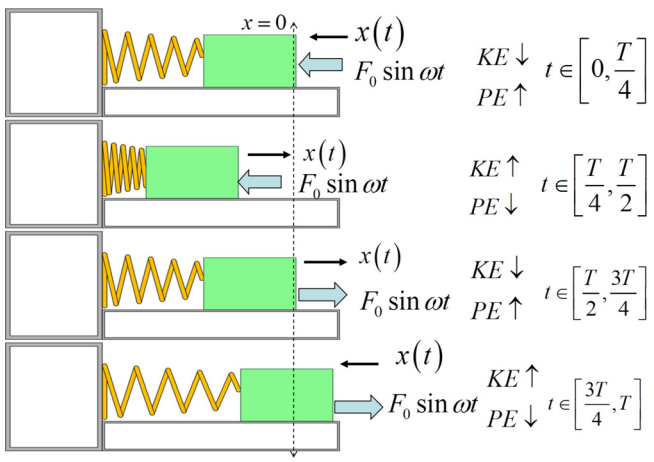


FIG. 11. The energy is bouncing between the mass and the source. When the driving force is pointing in the same direction as the displacement then work is supplied to the mass. This results in increase in its potential energy. After quarter of a cycle, this work is returned back to the source.

$$p(t) = F_D \frac{dx}{dt} = \frac{F_0^2 \omega}{2m(\omega_0^2 - \omega^2)} \sin 2\omega t. \tag{A5}$$

The instantaneous power is continuously changing from positive to negative. The sequence of events and how energy is transferred between the driving source and the mass-spring system is shown in Fig. 11. For the first quarter of a cycle, $t \in [0, T/4]$, the maximum kinetic energy together with the work exerted by the source is converted to the maximum potential energy at the end of the period. Then the potential energy will release its energy in two forms: kinetic energy to the mass and work back to the source. So, at $t = T/2$ all the work supplied by the source will return back to it. Then once the mass passes the equilibrium point ($x = 0$), where its kinetic energy is maximum, the source will supply the mass with energy so when the spring is fully stretched at $t = 3T/4$, the potential energy will return to its maximum value. This process repeats indefinitely.


[1]S. M. Mattar and S. Y. Elnaggar, J. Magn. Res. **209**, 174 (2011).
[2]S. Y. Elnaggar, R. Tervo, and S. M. Mattar, J. Magn. Res. **238**, 1 (2014).
[3]S. Y. Elnaggar, R. Tervo, and S. M. Mattar, J. Magn. Res. **242**, 57 (2014).
[4]S. Y. Elnaggar, R. Tervo, and S. M. Mattar, J. Magn. Res. **245**, 50 (2014).
[5]E. Shamonina, V. A. Kalinin, K. H. Ringhofer, and L. Solymar, J. Appl. Phys. **92**, 6252 (2002).
[6]R. R. A. Syms, E. Shamonina, and L. Solymar, Microwaves, IEE Proc. Antennas Propag. **153**, 111 (2006).
[7]A. Karalis, J. D. Joannopoulos, and M. Soljačić, Ann. Phys. **323**, 34 (2008).
[8]A. Kurs, A. Karalis, R. Moffatt, J. D. Joannopoulos, P. Fisher, and M. Soljačić, Science **317**, 83 (2007).
[9]Y. Zhuo, L. Yang, Z. Chao, and Y. Qingxin, IEEE Tran. Magn. **50**, 4004204 (2014).
[10]X. Yu, S. Sandhu, S. Beiker, R. Sassoon, and S. Fan, Appl. Phys. Lett. **99**, 214102 (2011).
[11]S. Kim, J. S. Ho, L. Y. Chen, and A. S. Y. Poon, Appl. Phys. Lett. **101**, 073701 (2012).
[12]N. Liu, H. Liu, S. Zhu, and H. Giessen, Nat. Photonics **3**, 157 (2009).
[13]V. V. Tyurnev, Prog. Electromagn. Res. B **21**, 47 (2010).
[14]V. V. Tyurnev, J. Commun. Technol. Electron. **47**, 1 (2002).
[15]I. Awai and Y. Zhang, Electron. Commun. Jpn. Part 2, Electron. **90**, 11 (2007).
[16]H. Jia-Sheng and M. J. Lancaster, IEEE Trans. Microwave Theory Tech. **44**, 2099 (1996).
[17]T. Kawaguchi and Y. Kobayashi, in *34th European Microwave Conference* (2004), Vol. 2, pp. 629–632.
[18]J. S. Hong, IEE Proc. Microwaves, Antennas Propag. **147**, 354 (2000).
[19]J. S. Hong, *Microstrip Filters for RF/Microwave Applications*, Wiley Series in Microwave and Optical Engineering, 2nd ed. (Wiley, New York, 2011).
[20]I. Awai, IECIE Trans. Electron. **E88-C**, 2295 (2005).
[21]D. A. Powell, M. Lapine, M. V. Gorkunov, I. V. Shadrivov, and Y. S. Kivshar, Phys. Rev. B **82**, 155128 (2010).
[22]D. A. Powell, K. Hannam, I. V. Shadrivov, and Y. S. Kivshar, Phys. Rev. B **83**, 235420 (2011).
[23]H. Liu, D. A. Genov, D. M. Wu, Y. M. Liu, Z. W. Liu, C. Sun, S. N. Zhu, and X. Zhang, Phys. Rev. B **76**, 073101 (2007).
[24]S. Elnaggar, R. Tervo, and S. Mattar, IEEE Trans. Microwave Theory Tech. **63**, 2115 (2015).
[25]R. J. Silbey and R. A. Alberty, *Physical Chemistry*, 3rd ed. (Wiley, 2000).
[26]S. Friedländer, O. Ovchar, H. Voigt, R. Böttcher, A. Belous, and A. Pöppl, Appl. Magn. Res. **46**(1), 33 (2014).
[27]D. M. Pozar, *Microwave Engineering*, 4th ed. (Wiley, 2011).

[28]J. D. Jackson, *Classical Electrodynamics* (John and Wiley Sons, 1962).
[29]J. B. Pendry, A. J. Holden, D. J. Robbins, and W. J. Stewart, IEEE Trans. Microwave Theory Tech. **47**, 2075 (1999).
[30]J. S. Hyde, W. Froncisz, and T. Oles, J. Magn. Res. **82**, 223 (1989).
[31]N. Liu and H. Giessen, Angew. Chem. Int. Ed. **49**, 9838 (2010).
[32]I. Sersic, M. Frimmer, E. Verhagen, and A. F. Koenderink, Phys. Rev. Lett. **103**, 213902 (2009).
[33]I. K. Kim and V. V. Varadan, J. Appl. Phys. **106**, 074504 (2009).
[34]L. Solymar and E. Shamonina, *Waves in Metamaterials* (Oxford University Press, 2009).
[35]H. Haus and W. P. Huang, Proc. IEEE **79**, 1505 (1991).
[36]S. B. Cohn, IEEE Trans. Microwave Theory Tech. **16**, 218 (1968).
[37]H. Liu, D. A. Genov, D. M. Wu, Y. M. Liu, J. M. Steele, C. Sun, S. N. Zhu, and X. Zhang, Phys. Rev. Lett. **97**, 243902 (2006).